MANIPULATING ATOMS WITH PHOTONS

Nobel Lecture, December 8, 1997

by

CLAUDE N. COHEN-TANNOUDJI

Collège de France et Laboratoire Kastler Brossel* de l'Ecole Normale Supérieure, 24 rue Lhomond, 75231 Paris Cedex 05, France

Electromagnetic interactions play a central role in low energy physics. They are responsible for the cohesion of atoms and molecules and they are at the origin of the emission and absorption of light by such systems. This light is not only a source of information on the structure of atoms. It can also be used to act on atoms, to manipulate them, to control their various degrees of freedom. With the development of laser sources, this research field has considerably expanded during the last few years. Methods have been developed to trap atoms and to cool them to very low temperatures. This has opened the way to a wealth of new investigations and applications.

Two types of degrees of freedom can be considered for an atom: the internal degrees of freedom, such as the electronic configuration or the spin polarization, in the center of mass system; the external degrees of freedom, which are essentially the position and the momentum of the center of mass. The manipulation of internal degrees of freedom goes back to optical pumping [1], which uses resonant exchanges of angular momentum between atoms and circularly polarized light for polarizing the spins of these atoms. These experiments predate the use of lasers in atomic physics. The manipulation of external degrees of freedom uses the concept of radiative forces resulting from the exchanges of linear momentum between atoms and light. Radiative forces exerted by the light coming from the sun were already invoked by J. Kepler to explain the tails of the comets. Although they are very small when one uses ordinary light sources, these forces were also investigated experimentally in the beginning of this century by P. Lebedev, E. F. Nichols and G. F. Hull, R. Frisch. For a historical survey of this research field, we refer the reader to review papers [2, 3, 4, 5] which also include a discussion of early theoretical work dealing with these problems by the groups of A. P. Kazantsev, V. S. Letokhov, in Russia, A. Ashkin at Bell Labs, S. Stenholm in Helsinki.

It turns out that there is a strong interplay between the dynamics of internal and external degrees of freedom. This is at the origin of efficient laser cooling mechanisms, such as "Sisyphus cooling" or "Velocity Selective Cohe-

* Laboratoire Kastler Brossel is a Laboratoire associé au CNRS et à l'Université Pierre et Marie Curie.

rent Population Trapping", which were discovered at the end of the 80's (for a historical survey of these developments, see for example [6]). These mechanisms have allowed laser cooling to overcome important fundamental limits, such as the Doppler limit and the single photon recoil limit, and to reach the microKelvin, and even the nanoKelvin range. We devote a large part of this paper (sections 2 and 3) to the discussion of these mechanisms and to the description of a few applications investigated by our group in Paris (section 4). There is a certain continuity between these recent developments in the field of laser cooling and trapping and early theoretical and experimental work performed in the 60's and the 70's, dealing with internal degrees of freedom. We illustrate this continuity by presenting in section 1 a brief survey of various physical processes, and by interpreting them in terms of two parameters, the radiative broadening and the light shift of the atomic ground state.

1. BRIEF REVIEW OF PHYSICAL PROCESSES

To classify the basic physical processes which are used for manipulating atoms by light, it is useful to distinguish two large categories of effects: dissipative (or absorptive) effects on the one hand, reactive (or dispersive) effects on the other hand. This partition is relevant for both internal and external degrees of freedom.

1.1 EXISTENCE OF TWO TYPES OF EFFECTS IN ATOM-PHOTON INTERACTIONS

Consider first a light beam with frequency ω_L propagating through a medium consisting of atoms with resonance frequency ω_A. The index of refraction describing this propagation has an imaginary part and a real part which are associated with two types of physical processes. The incident photons can be absorbed, more precisely scattered in all directions. The corresponding attenuation of the light beam is maximum at resonance. It is described by the imaginary part of the index of refraction which varies with $\omega_L-\omega_A$ as a Lorentz absorption curve. We will call such an effect a dissipative (or absorptive) effect. The speed of propagation of light is also modified. The corresponding dispersion is described by the real part n of the index of refraction whose difference from 1, $n-1$, varies with $\omega_L-\omega_A$ as a Lorentz dispersion curve. We will call such an effect a reactive (or dispersive) effect.

Dissipative effects and reactive effects also appear for the atoms, as a result of their interaction with photons. They correspond to a broadening and to a shift of the atomic energy levels, respectively. Such effects already appear when the atom interacts with the quantized radiation field in the vacuum state. It is well known that atomic excited states get a natural width Γ, which is also the rate at which a photon is spontaneously emitted from such states. Atomic energy levels are also shifted as a result of virtual emissions and reabsorptions of photons by the atom. Such a radiative correction is simply the Lamb shift [7].

Similar effects are associated with the interaction with an incident light beam. Atomic ground states get a radiative broadening Γ', which is also the rate at which photons are absorbed by the atom, or more precisely scattered from the incident beam. Atomic energy levels are also shifted as a result of virtual absorptions and reemissions of the incident photons by the atom. Such energy displacements $\hbar\Delta'$ are called light shifts, or ac Stark shifts [8, 9].

In view of their importance for the following discussions, we give now a brief derivation of the expressions of Γ' and Δ', using the so-called dressed-atom approach to atom-photon interactions (see for example [10], chapter VI). In the absence of coupling, the two dressed states $|g, N\rangle$ (atom in the ground state g in the presence of N photons) and $|e, N-1\rangle$ (atom in the excited state e in the presence of $N-1$ photons) are separated by a splitting $\hbar\delta$, where $\delta = \omega_L - \omega_A$ is the detuning between the light frequency ω_L and the atomic frequency ω_A. The atom-light interaction Hamiltonian V_{AL} couples these two states because the atom in g can absorb one photon and jump to e. The corresponding matrix element of V_{AL} can be written as $\hbar\Omega/2$, where the so-called Rabi frequency Ω is proportional to the transition dipole moment and to $\sqrt{N}$. Under the effect of such a coupling, the two states repel each other, and the state $|g, N\rangle$ is shifted by an amount $\hbar\Delta'$, which is the light shift of g. The contamination of $|g, N\rangle$ by the unstable state $|e, N-1\rangle$ (having a width Γ) also confers to the ground state a width Γ'. In the limit where $\Omega \ll \Gamma$ or $|\delta|$, a simple perturbative calculation gives:

$$\Gamma' = \Omega^2 \frac{\Gamma}{\Gamma^2 + 4\delta^2} \tag{1}$$

$$\Delta' = \Omega^2 \frac{\delta}{\Gamma^2 + 4\delta^2} \tag{2}$$

Both Γ' and Δ' are proportional to $\Omega^2 \propto N$, *i.e.* to the light intensity. They vary with the detuning $\delta = \omega_L - \omega_A$ as Lorentz absorption and dispersion curves, respectively, which justifies the denominations absorptive and dispersive used for these two types of effects. For large detunings ($|\delta| \gg \Gamma$), Γ' varies as $1/\delta^2$ and becomes negligible compared to Δ' which varies as $1/\delta$. On the other hand, for small detunings, ($|\delta| \ll \Gamma$), Γ' is much larger than Δ'. In the high intensity limit, when Ω is large compared to Γ and $|\delta|$, the two dressed states resulting from the coupling are the symmetric and antisymmetric linear combinations of $|g, N\rangle$ and $|e, N-1\rangle$. Their splitting is $\hbar\Omega$ and they share the instability Γ of e in equal parts, so that $\Gamma' = \Gamma/2$. One can explain in this way various physical effects such as the Rabi flopping or the Autler-Townes splittings of the spectral lines connecting e or g to a third level [11].

1.2 *MANIPULATION OF INTERNAL DEGREES OF FREEDOM*

1.2.1 *Optical pumping*

Optical pumping is one of the first examples of manipulation of atoms by light [1]. It uses resonant excitation of atoms by circularly polarized light for transferring to the atoms part of the angular momentum carried by the light

beam. It is based on the fact that different Zeeman sublevels in the atomic ground state have in general different absorption rates for incoming polarized light. For example, for a $J_g = 1/2 \leftrightarrow J_e = 1/2$ transition, only atoms in the sublevel $M_g = -1/2$ can absorb σ^+-polarized light. They are excited in the sublevel $M_e = +1/2$ of e from which they can fall back in the sublevel $M_g = +1/2$ by spontaneous emission of a π-polarized photon. They then remain trapped in this state because no further σ^+-transition can take place. It is possible in this way to obtain high degrees of spin orientation in atomic ground states.

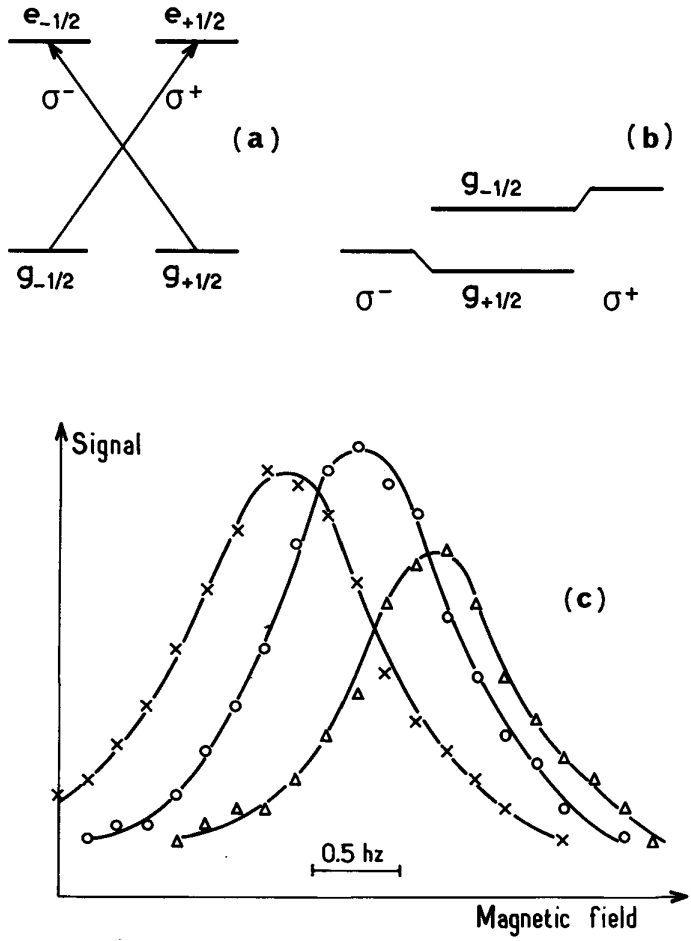

Figure 1. Experimental observation of light shifts (from reference [12]). For a $J_g = 1/2 \leftrightarrow J_e = 1/2$ transition (a), a σ^+-polarized non-resonant excitation shifts only the sublevel $g_{-1/2}$ (right part of b), whereas a σ^--polarized excitation shifts only the sublevel $g_{+1/2}$ (left part of b). The detuning δ is positive and very large compared to the Zeeman splittings in e and g. The Zeeman splitting in the ground state is thus increased in the first case, decreased in the second one. (c) magnetic resonance signal versus magnetic field, in units of the corresponding Larmor frequency. The central curve (circles) is the resonance curve in the absence of light shift. When the non-resonant light beam is introduced, either σ^+-polarized (crosses) or σ^--polarized (triangles) the magnetic resonance curve is light shifted in opposite directions.

1.2.2 *Light shifts*

Optical pumping is a dissipative effect because it is associated with resonant absorption of photons by the atom. Non-resonant optical excitation produces light shifts of the ground state Zeeman sublevels. Because of the polarization selection rules, light shifts depend on the polarization of the exciting light and vary in general from one Zeeman sublevel to another. Consider for example a $J_g = 1/2 \leftrightarrow J_e = 1/2$ transition (Fig.1a). A σ^+-polarized excitation shifts only the Zeeman sublevel $M_g = -1/2$, whereas a σ^--polarized excitation shifts only the sublevel $M_g = +1/2$ (Fig.1b). Magnetic resonance curves in the ground state g which are very narrow because the relaxation time in g can be very long, are thus light shifted by a polarized non-resonant excitation, and the sign of this shift changes when one changes the polarization of the light beam from σ^+ to σ^-. It is in this way that light shifts were first observed [12]. Fig.1c gives an example of experimental results obtained by exciting the transition 6^1S_0, $F = 1/2 \leftrightarrow 6^3P_1$, $F = 1/2$ of ^{199}Hg atoms by the non-resonant light coming from a lamp filled with another isotope (^{201}Hg).

Light shifts can be considered from different points of view. First, they can be interpreted as a radiative correction, due to the interaction of the atom with an incident field rather than with the vacuum field. This is why Alfred Kastler called them "Lamp shifts". Secondly, they introduce perturbations to high precision measurements using optical methods, which must be taken into account before extracting spectroscopic data from these measurements. Finally, because of their variation from one sublevel to another, the effect of light shifts can be described in terms of fictitious magnetic or electric fields [13]. This explains why the light shifts produced by a non-resonant laser standing wave are being more and more frequently used to produce spatial modulations of the Zeeman splittings in the ground state on an optical wavelength scale. This would not be easily achieved with spatially varying real magnetic fields. We will see in section 2 interesting applications of such a situation.

1.3 *MANIPULATION OF EXTERNAL DEGREES OF FREEDOM*

1.3.1 *The two types of radiative forces*

There are two types of radiative forces, associated with dissipative and reactive effects respectively.

Dissipative forces, also called radiation pressure forces or scattering forces, are associated with the transfer of linear momentum from the incident light beam to the atom in resonant scattering processes. They are proportional to the scattering rate Γ'. Consider for example an atom in a laser plane wave with wave vector $\mathbf{k}$. Because photons are scattered with equal probabilities in two opposite directions, the mean momentum transferred to the atom in an absorption-spontaneous emission cycle is equal to the momentum $\hbar\mathbf{k}$ of the absorbed photon. The mean rate of momentum transfer, *i.e.* the mean force, is thus equal to $\hbar\mathbf{k}\Gamma'$. Since Γ' saturates to $\Gamma/2$ at high intensity (see section 1.1), the radiation pressure force saturates to $\hbar\mathbf{k}\Gamma/2$. The corresponding acceleration (or deceleration) which can be communicated to an atom with

mass M, is equal to $a_{max} = \hbar k\Gamma/2M = v_R/2\tau$, where $v_R = \hbar k/M$ is the recoil velocity of the atom absorbing or emitting a single photon, and $\tau = 1/\Gamma$ is the radiative lifetime of the excited state. For sodium atoms, $v_R = 3 \times 10^{-2}$ m/s and $\tau = 1.6 \times 10^{-8}$ s, so that a_{max} can reach values as large as 10^6 m/s^2, *i.e.* $10^5 g$ where g is the acceleration due to gravity. With such a force, one can stop a thermal atomic beam in a distance of the order of one meter, provided that one compensates for the Doppler shift of the decelerating atom, by using for example a spatially varying Zeeman shift [14, 15] or a chirped laser frequency [16].

Dispersive forces, also called dipole forces or gradient forces [2, 3, 17], can be interpreted in terms of position dependent light shifts $\hbar\Delta'(\mathbf{r})$ due to a spatially varying light intensity [18]. Consider for example a laser beam well detuned from resonance, so that one can neglect Γ' (no scattering process). The atom thus remains in the ground state and the light shift $\hbar\Delta'(\mathbf{r})$ of this state plays the role of a potential energy, giving rise to a force which is equal and opposite to its gradient : $\mathbf{F} = -\nabla[\hbar\Delta'(\mathbf{r})]$. Such a force can also be interpreted as resulting from a redistribution of photons between the various plane waves forming the laser wave in absorption-stimulated emission cycles. If the detuning is not large enough to allow Γ' to be neglected, spontaneous transitions occur between dressed states having opposite gradients, so that the instantaneous force oscillates back and forth between two opposite values in a random way. Such a dressed atom picture provides a simple interpretation of the mean value and of the fluctuations of dipole forces [19].

1.3.2 *Applications of dissipative forces – Doppler cooling and magneto-optical traps*

We have already mentioned in the previous subsection the possibility of decelerating an atomic beam by the radiation pressure force of a laser plane wave. Interesting effects can also be obtained by combining the effects of two counterpropagating laser waves.

A first example is Doppler cooling, first suggested for neutral atoms by T. W. Hänsch and A.L. Schawlow [20] and, independently for trapped ions, by D. Wineland and H. Dehmelt [21]. This cooling process results from a Doppler induced imbalance between two opposite radiation pressure forces. The two counterpropagating laser waves have the same (weak) intensity and the same frequency and they are slightly detuned to the red of the atomic frequency ($\omega_L < \omega_A$). For an atom at rest, the two radiation pressure forces exactly balance each other and the net force is equal to zero. For a moving atom, the apparent frequencies of the two laser waves are Doppler shifted. The counterpropagating wave gets closer to resonance and exerts a stronger radiation pressure force than the copropagating wave which gets farther from resonance. The net force is thus opposite to the atomic velocity v and can be written for small v as $F = -\alpha v$ where α is a friction coefficient. By using three pairs of counterpropagating laser waves along three orthogonal directions, one can damp the atomic velocity in a very short time, on the order of a few microseconds, achieving what is called an "optical molasses" [22].

The Doppler friction responsible for the cooling is necessarily accompanied by fluctuations due to the fluorescence photons which are spontaneously emitted in random directions and at random times. These photons communicate to the atom a random recoil momentum $\hbar k$, responsible for a momentum diffusion described by a diffusion coefficient D [3, 18, 25]. As in usual Brownian motion, competition between friction and diffusion usually leads to a steady-state, with an equilibrium temperature proportional to D/α. The theory of Doppler cooling [23, 24, 25] predicts that the equilibrium temperature obtained with such a scheme is always larger than a certain limit T_D, called the Doppler limit, and given by $k_B T_D = \hbar\Gamma/2$ where Γ is the natural width of the excited state and k_B the Boltzmann constant. This limit, which is reached for $\delta = \omega_L - \omega_A = -\Gamma/2$, is, for alkali atoms, on the order of 100 μK. In fact, when the measurements became precise enough, it appeared that the temperature in optical molasses was much lower than expected [26]. This indicates that other laser cooling mechanisms, more powerful than Doppler cooling, are operating. We will come back to this point in section 2.

The imbalance between two opposite radiation pressure forces can be also made position dependent though a spatially dependent Zeeman shift produced by a magnetic field gradient. In a one-dimensional configuration, first suggested by J. Dalibard in 1986, the two counterpropagating waves, which are detuned to the red ($\omega_L < \omega_A$) and which have opposite circular polarizations are in resonance with the atom at different places. This results in a restoring force towards the point where the magnetic field vanishes. Furthermore the non zero value of the detuning provides a Doppler cooling. In fact, such a scheme can be extended to three dimensions and leads to a robust, large and deep trap called "magneto-optical trap" or "MOT" [27]. It combines trapping and cooling, it has a large velocity capture range and it can be used for trapping atoms in a small cell filled with a low pressure vapour [28].

1.3.3 *Applications of dispersive forces : laser traps and atomic mirrors*

When the detuning is negative ($\omega_L - \omega_A < 0$), light shifts are negative. If the laser beam is focussed, the focal zone where the intensity is maximum appears as a minimum of potential energy, forming a potential well where sufficiently cold atoms can be trapped. This is a laser trap. Laser traps using a single focussed laser beam [29] or two crossed focussed laser beams [30, 31] have been realized. Early proposals [32] were considering trapping atoms at the antinodes or nodes of a non resonant laser standing wave. Channeling of atoms in a laser standing wave has been observed experimentally [33].

If the detuning is positive, light shifts are positive and can thus be used to produce potential barriers. For example an evanescent blue detuned wave at the surface of a piece of glass can prevent slow atoms impinging on the glass surface from touching the wall, making them bounce off a "carpet of light" [34]. This is the principle of mirrors for atoms. Plane atomic mirrors [35, 36] have been realized as well as concave mirrors [37].

2. SUB-DOPPLER COOLING

In the previous section, we discussed separately the manipulation of internal and external degrees of freedom, and we have described physical mechanisms involving only one type of physical effect, either dispersive or dissipative. In fact, there exist cooling mechanisms resulting from an interplay between spin and external degrees of freedom, and between dispersive and dissipative effects. We discuss in this section one of them, the so-called "Sisyphus cooling" or "polarization-gradient cooling" mechanism [38, 39] (see also [19]), which leads to temperatures much lower than Doppler cooling. One can understand in this way the sub-Doppler temperatures observed in optical molasses and mentioned above in section 1.3.2.

2.1 *SISYPHUS EFFECT*

Most atoms, in particular alkali atoms, have a Zeeman structure in the ground state. Since the detuning used in laser cooling experiments is not too large compared to Γ, both differential light shifts and optical pumping transitions exist for the various ground state Zeeman sublevels. Furthermore, the laser polarization varies in general in space so that light shifts and optical pumping rates are position-dependent. We show now, with a simple one-dimensional example, how the combination of these various effects can lead to a very efficient cooling mechanism.

Consider the laser configuration of Fig.2a, consisting of two counterpropagating plane waves along the z-axis, with orthogonal linear polarizations and with the same frequency and the same intensity. Because the phase shift between the two waves increases linearly with z, the polarization of the total field changes from σ^+ to σ^- and vice versa every $\lambda/4$. In between, it is elliptical or linear.

Consider now the simple case where the atomic ground state has an angular momentum $J_g = 1/2$. As shown in subsection (1.2), the two Zeeman sublevels $M_g = \pm 1/2$ undergo different light shifts, depending on the laser polarization, so that the Zeeman degeneracy in zero magnetic field is removed. This gives the energy diagram of Fig.2b showing spatial modulations of the Zeeman splitting between the two sublevels with a period $\lambda/2$.

If the detuning δ is not too large compared to Γ, there are also real absorptions of photons by the atom followed by spontaneous emission, which give rise to optical pumping transfers between the two sublevels, whose direction depends on the polarization: $M_g = -1/2 \rightarrow M_g = +1/2$ for a σ^+ polarization, $M_g = +1/2 \rightarrow M_g = -1/2$ for a σ^- polarization. Here also, the spatial modulation of the laser polarization results in a spatial modulation of the optical pumping rates with a period $\lambda/2$ (vertical arrows of Fig.2b).

The two spatial modulations of light shifts and optical pumping rates are of course correlated because they are due to the same cause, the spatial modulation of the light polarization. These correlations clearly appear in Fig.2b. With the proper sign of the detuning, optical pumping always transfers atoms from the higher Zeeman sublevel to the lower one. Suppose now that the

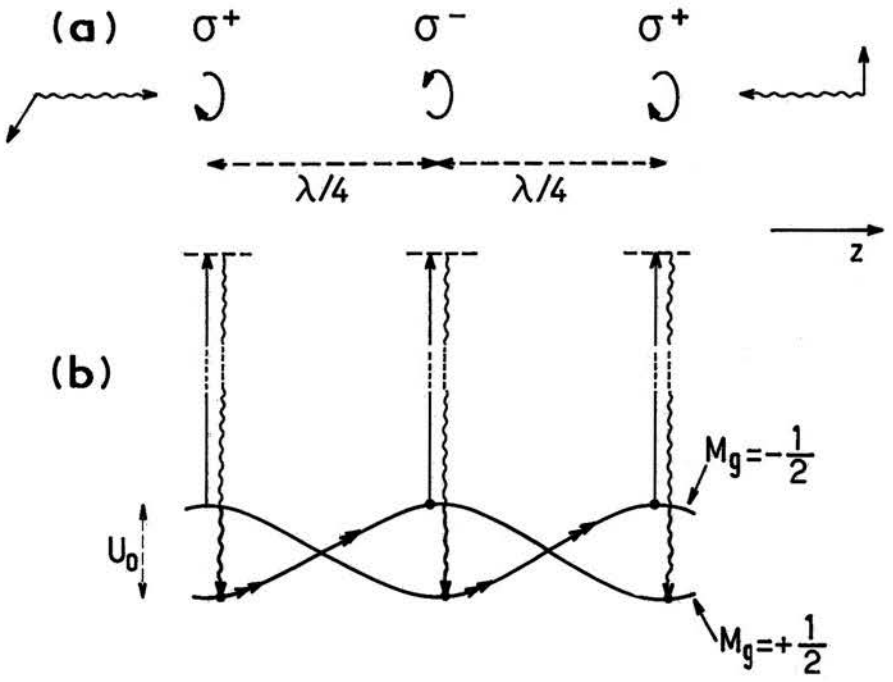

Figure 2. Sisyphus cooling. Laser configuration formed by two counterpropagating plane waves along the z-axis with orthogonal linear polarizations (a). The polarization of the resulting electric field is spatially modulated with a period $\lambda/2$. Every $\lambda/4$, it changes from σ^+ to σ^- and vice versa. For an atom with two ground state Zeeman sublevels $M_g = \pm 1/2$, the spatial modulation of the laser polarization results in correlated spatial modulations of the light shifts of these two sublevels and of the optical pumping rates between them (b). Because of these correlations, a moving atom runs up potential hills more frequently than down (double arrows of b).

atom is moving to the right, starting from the bottom of a valley, for example in the state $M_g = +1/2$ at a place where the polarization is σ^+. Because of the finite value of the optical pumping time, there is a time lag between internal and external variables and the atom can climb up the potential hill before absorbing a photon and reach the top of the hill where it has the maximum probability to be optically pumped in the other sublevel, i.e. in the bottom of a valley, and so on (double arrows of Fig.2b). Like Sisyphus in the Greek mythology, who was always rolling a stone up the slope, the atom is running up potential hills more frequently than down. When it climbs a potential hill, its kinetic energy is transformed into potential energy. Dissipation then occurs by light, since the spontaneously emitted photon has an energy higher than the absorbed laser photon (anti-Stokes Raman processes of Fig.2b). After each Sisyphus cycle, the total energy E of the atom decreases by an amount of the order of U_0, where U_0 is the depth of the optical potential wells of Fig.2b, until E becomes smaller than U_0, in which case the atom remains trapped in the potential wells.

The previous discussion shows that Sisyphus cooling leads to temperatures T_{Sis} such that $k_B T_{\text{Sis}} \simeq U_0$. According to Eq. (2), the light shift U_0 is proportional to $\hbar\Omega^2/\delta$ when $4|\delta| > \Gamma$. Such a dependence of T_{Sis} on the Rabi frequen-

cy Ω and on the detuning δ has been checked experimentally with cesium atoms [40]. Fig.3 presents the variations of the measured temperature T with the dimensionless parameter $\Omega^2/\Gamma|\delta|$. Measurements of T versus intensity for different values of δ show that T depends linearly, for low enough intensities, on a single parameter which is the light shift of the ground state Zeeman sublevels.

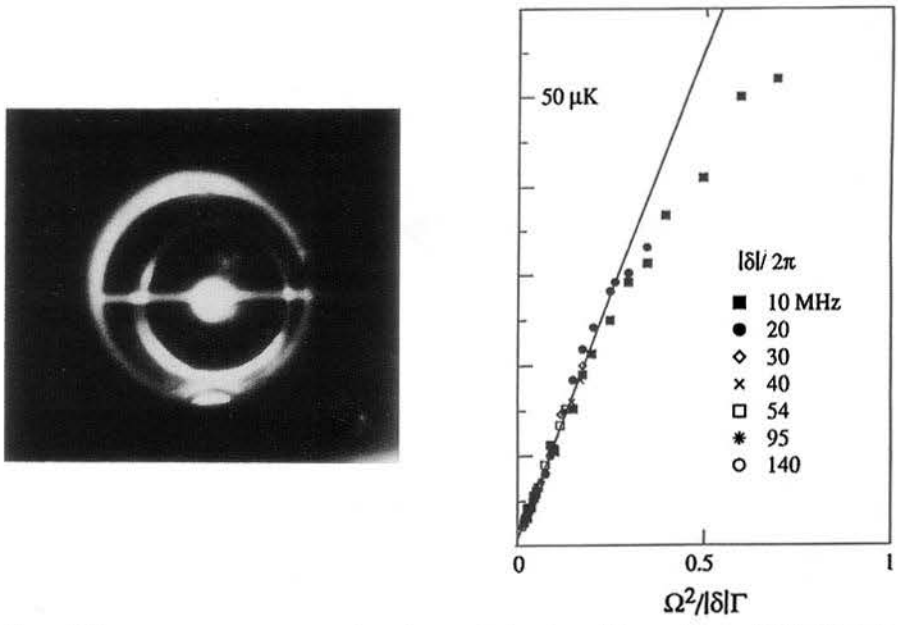

Figure 3. Temperature measurements in cesium optical molasses (from reference [40]). The left part of the figure shows the fluorescence light emitted by the molasses observed through a window of the vacuum chamber. The horizontal bright line is the fluorescence light emitted by the atomic beam which feeds the molasses and which is slowed down by a frequency chirped laser beam. Right part of the figure : temperature of the atoms measured by a time of flight technique versus the dimensionless parameter $\Omega^2/|\delta|\Gamma$ proportional to the light shift (Ω is the optical Rabi frequency, δ the detuning and Γ the natural width of the excited state).

2.2 *THE LIMITS OF SISYPHUS COOLING*

At low intensity, the light shift $U_0 \propto \hbar\Omega^2/\delta$ is much smaller than $\hbar\Gamma$. This explains why Sisyphus cooling leads to temperatures much lower than those achievable with Doppler cooling. One cannot however decrease indefinitely the laser intensity. The previous discussion ignores the recoil due to the spontaneously emitted photons which increases the kinetic energy of the atom by an amount on the order of E_R, where

$$E_R = \hbar^2 k^2/2M \tag{3}$$

is the recoil energy of an atom absorbing or emitting a single photon. When U_0 becomes on the order or smaller than E_R, the cooling due to Sisyphus cooling becomes weaker than the heating due to the recoil, and Sisyphus cooling no longer works. This shows that the lowest temperatures which can

be achieved with such a scheme are on the order of a few E_R/k_B. This result is confirmed by a full quantum theory of Sisyphus cooling [41, 42] and is in good agreement with experimental results. The minimum temperature in Fig.3 is on the order of $10E_R/k_B$.

2.3 *OPTICAL LATTICES*

For the optimal conditions of Sisyphus cooling, atoms become so cold that they get trapped in the quantum vibrational levels of a potential well (see Fig. 4). More precisely, one must consider energy bands in this perodic structure [43]. Experimental observation of such a quantization of atomic motion

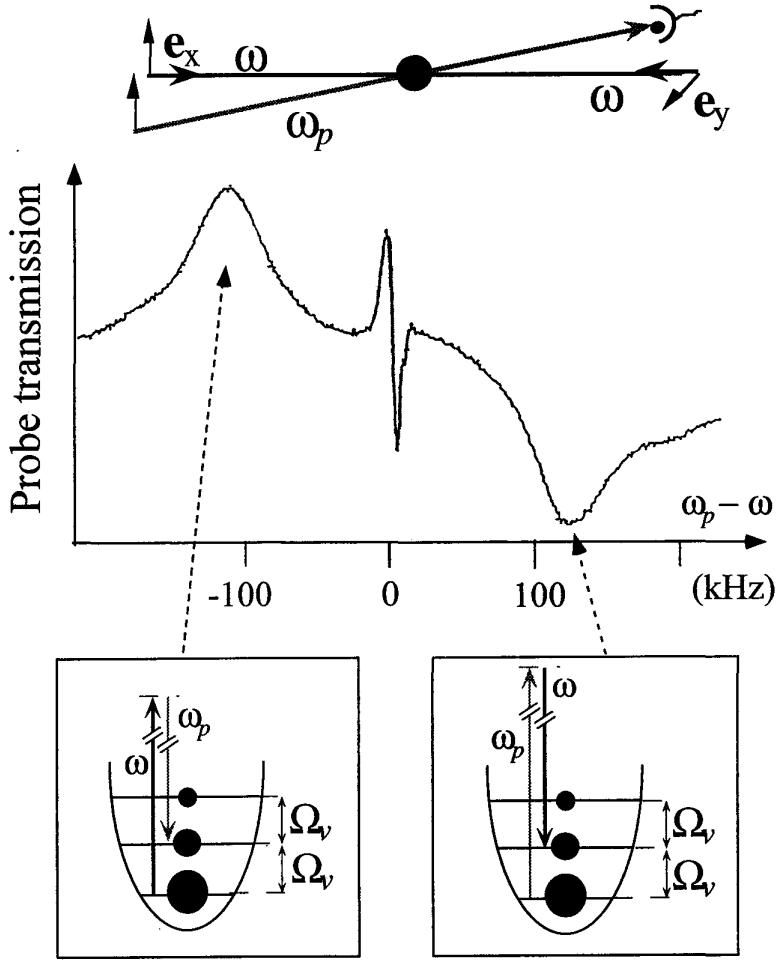

Figure 4. Probe absorption spectrum of a 1-D optical lattice (from reference [44]). The upper part of the figure shows the two counterpropagating laser beams with frequency ω and orthogonal linear polarizations forming the 1D-optical lattice, and the probe beam with frequency ω_p whose absorption is measured by a detector. The lower part of the figure shows the probe transmission versus ω_p–ω. The two lateral resonances corresponding to amplification or absorption of the probe are due to stimulated Raman processes between vibrational levels of the atoms trapped in the light field (see the two insets). The central narrow structure is a Rayleigh line due to the antiferromagnetic spatial order of the atoms.

in an optical potential was first achieved in one dimension [44] [45]. Atoms are trapped in a spatial periodic array of potential wells, called a "1D-optical lattice", with an antiferromagnetic order, since two adjacent potential wells correspond to opposite spin polarizations. 2D and 3D optical lattices have been realized subsequently (see the review papers [46] [47]).

3. SUBRECOIL LASER COOLING

3.1 *THE SINGLE PHOTON RECOIL LIMIT. HOW TO CIRCUMVENT IT*

In most laser cooling schemes, fluorescence cycles never cease. Since the random recoil $\hbar k$ communicated to the atom by the spontaneously emitted photons cannot be controlled, it seems impossible to reduce the atomic momentum spread δp below a value corresponding to the photon momentum $\hbar k$. Condition $\delta p = \hbar k$ defines the "single photon recoil limit". It is usual in laser cooling to define an effective temperature T in terms of the half-width δp (at $1/\sqrt{e}$) of the momentum distribution by $k_B T/2 = \delta p^2/2M$. In the temperature scale, condition $\delta p = \hbar k$ defines a "recoil temperature" T_R by:

$$\frac{k_B T_R}{2} = \frac{\hbar^2 k^2}{2M} = E_R \tag{4}$$

The value of T_R ranges from a few hundred nanoKelvin for alkalis to a few microKelvin for helium.

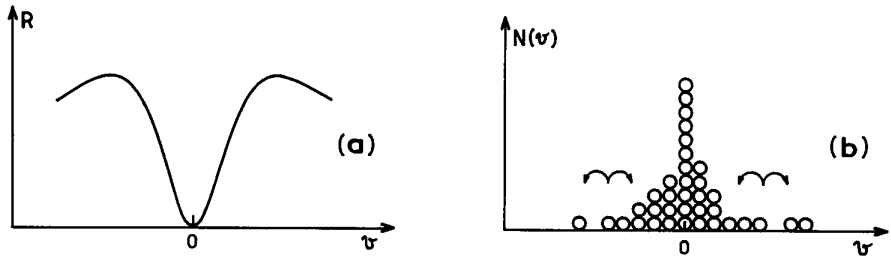

Figure 5. Subrecoil laser cooling. The random walk of the atom in velocity space is supposed to be characterized by a jump rate R which vanishes for $v = 0$ (a). As a result of this inhomogeneous random walk, atoms which fall in a small interval around $v = 0$ remain trapped there for a long time, on the order of $[R(v)]^{-1}$, and accumulate (b).

It is in fact possible to circumvent this limit and to reach temperatures T lower than T_R, a regime which is called "subrecoil" laser cooling. The basic idea is to create a situation where the photon absorption rate Γ', which is also the jump rate R of the atomic random walk in velocity space, depends on the atomic velocity $v = p/M$ and vanishes for $v = 0$ (Fig.5a). Consider then an atom with $v = 0$. For such an atom, the absorption of light is quenched. Consequently, there is no spontaneous reemission and no associated random recoil. One protects in this way ultracold atoms (with $v \simeq 0$) from the "bad" effects of the light. On the other hand, atoms with $v \neq 0$ can absorb and reemit light. In such absorption-spontaneous emission cycles, their velocities change in a random way and the corresponding random walk in v-space can transfer

atoms from the $v \neq 0$ absorbing states into the $v \simeq 0$ dark states where they remain trapped and accumulate (see Fig. 5b). This reminds us of what happens in a Kundt's tube where sand grains vibrate in an acoustic standing wave and accumulate at the nodes of this wave where they no longer move. Note however that the random walk takes place in velocity space for the situation considered in Fig. 5b, whereas it takes place in position space in a Kundt's tube.

Up to now, two subrecoil cooling schemes have been proposed and demonstrated. In the first one, called "Velocity Selective Coherent Population Trapping" (VSCPT), the vanishing of $R(v)$ for $v = 0$ is achieved by using destructive quantum interference between different absorption amplitudes [48]. The second one, called Raman cooling, uses appropriate sequences of stimulated Raman and optical pumping pulses for tailoring the appropriate shape of $R(v)$ [49].

3.2 *BRIEF SURVEY OF VSCPT*

We first recall the principle of the quenching of absorption by "coherent population trapping", an effect which was discovered and studied in 1976 [50, 51]. Consider the 3-level system of Fig.6, with two ground state sublevels g_1 and g_2 and one excited sublevel e_0, driven by two laser fields with frequencies ω_{L1} and ω_{L2}, exciting the transitions $g_1 \leftrightarrow e_0$ and $g_2 \leftrightarrow e_0$, respectively. Let $\hbar\Delta$ be the detuning from resonance for the stimulated Raman process consisting of the absorption of one ω_{L1} photon and the stimulated emission of one ω_{L2} photon, the atom going from g_1 to g_2. One observes that the fluorescence

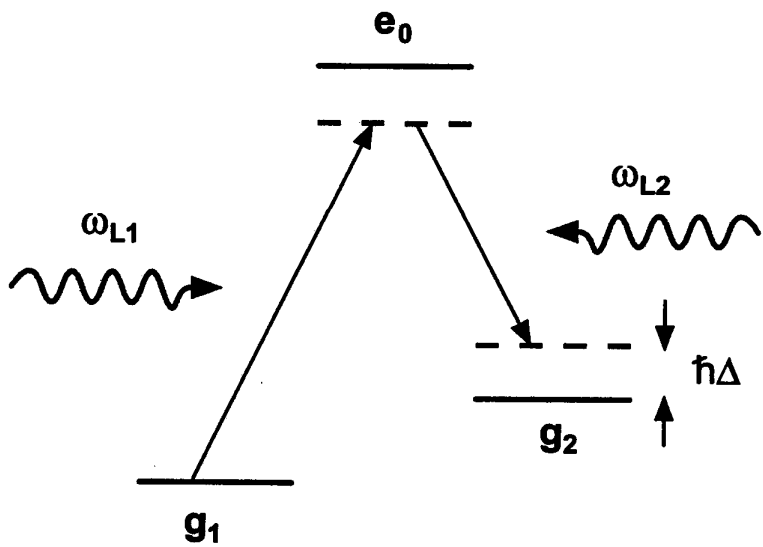

Figure 6. Coherent population trapping. A three-level atom g_1, g_2, e_0 is driven by two laser fields with frequences ω_{L1} and ω_{L2} exciting the transitions $g_1 \leftrightarrow e_0$ and $g_2 \leftrightarrow e_0$, respectively. $\hbar\Delta$ is the detuning from resonance for the stimulated Raman process induced between g_1 and g_2 by the two laser fields ω_{L1} and ω_{L2}. When $\Delta = 0$, atoms are optically pumped in a linear superposition of g_1 and g_2 which no longer absorbs light because of a destructive interference between the two absorption amplitudes $g_1 \rightarrow e_0$ and $g_2 \rightarrow e_0$.

rate R vanishes for $\Delta = 0$. Plotted versus Δ, the variations of R are similar to those of Fig.5a with v replaced by Δ. The interpretation of this effect is that atoms are optically pumped into a linear superposition of g_1 and g_2 which is not coupled to e_0 because of a destructive interference between the two absorption amplitudes $g_1 \rightarrow e_0$ and $g_2 \rightarrow e_0$.

The basic idea of VSCPT is to use the Doppler effect for making the detuning Δ of the stimulated Raman process of Fig.6 proportional to the atomic velocity v. The quenching of absorption by coherent population trapping is thus made velocity dependent and one achieves the situation of Fig. 5.a. This is obtained by taking the two laser waves ω_{L1} and ω_{L2} counterpropagating along the z-axis and by choosing their frequencies in such a way that $\Delta = 0$ for an atom at rest. Then, for an atom moving with a velocity v along the z-axis, the opposite Doppler shifts of the two laser waves result in a Raman detuning $\Delta = (k_1 + k_2)\, v$ proportional to v.

A more quantitative analysis of the cooling process [52] shows that the dark state, for which $R = 0$, is a linear superposition of two states which differ not only by the internal state (g_1 or g_2) but also by the momentum along the z-axis:

$$|\psi_D\rangle = c_1\, |g_1, -\hbar k_1\rangle + c_2\, |g_2, +\hbar k_2\rangle \tag{5}$$

This is due to the fact that g_1 and g_2 must be associated with different momenta, $-\hbar k_1$ and $+\hbar k_2$, in order to be coupled to the same excited state $|e_0, p = 0\rangle$ by absorption of photons with different momenta $+\hbar k_1$ and $-\hbar k_2$. Furthermore, when $\Delta = 0$, the state (5) is a stationary state of the total atom + laser photons system. As a result of the cooling by VSCPT, the atomic momentum distribution thus exhibits two sharp peaks, centered at $-\hbar k_1$ and

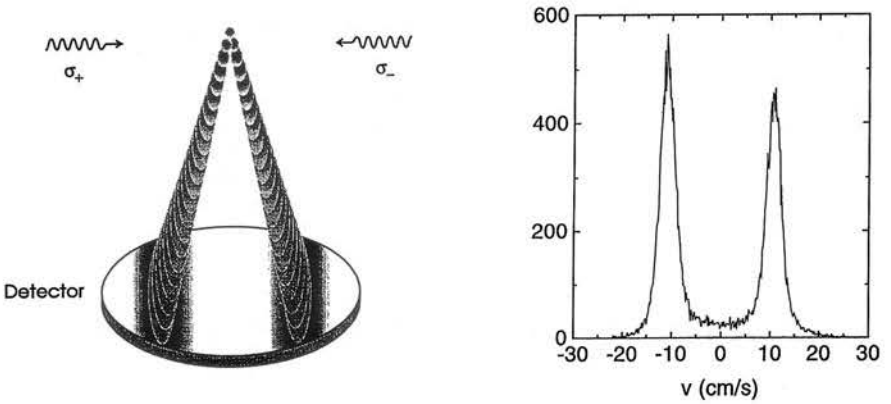

Figure 7. One-dimensional VSCPT experiment. The left part of the figure shows the experimental scheme. The cloud of precooled trapped atoms is released while the two counterpropagating VSCPT beams with orthogonal circular polarizations are applied during a time $\theta = 1$ms. The atoms then fall freely and their positions are detected 6.5 cm below on a microchannel plate. The double band pattern is a signature of the 1D cooling process which accumulates the atoms in a state which is a linear superposition of two different momenta. The right part of the figure gives the velocity distribution of the atoms detected by the microchannel plate. The width δv of the two peaks is clearly smaller than their separation $2v_R$, where $v_R = 9.2$ cm/s is the recoil velocity. This is a clear signature of subrecoil cooling.

$+\hbar k_2$, with a width δp which tends to zero when the interaction time Θ tends to infinity.

The first VSCPT experiment [48] was performed on the 2^3S_1 metastable state of helium atoms. The two lower states g_1 and g_2 were the $M = -1$ and $M = +1$ Zeeman sublevels of the 2^3S_1 metastable state, e_0 was the $M = 0$ Zeeman sublevel of the excited 2^3P_1 state. The two counterpropagating laser waves had the same frequency $\omega_{L1} = \omega_{L2} = \omega_L$ and opposite circular polarizations. The two peaks of the momentum distribution were centered at $\pm\hbar k$, with a width corresponding to $T \simeq T_R/2$. The interaction time was then increased by starting from a cloud of trapped precooled helium atoms instead of using an atomic beam as in the first experiment [53]. This led to much lower temperatures (see Fig. 8). Very recently, temperatures as low as $T_R/800$ have been observed [54].

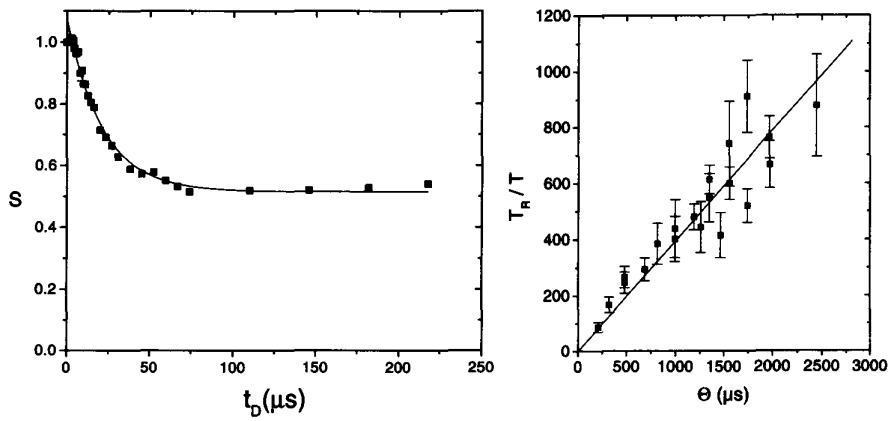

Figure 8. Measurement of the spatial correlation function of atoms cooled by VSCPT (from reference [54]). After a cooling period of duration θ, the two VSCPT beams are switched off during a dark period of duration t_D. The two coherent wave packets into which atoms are pumped fly apart with a relative velocity $2v_R$ and get separated by a distance $a = 2v_R t_D$. Reapplying the two VSCPT beams during a short probe pulse, one measures a signal S which can be shown to be equal to $[1 + G(a)]/2$ where $G(a)$ is the spatial overlap between the two identical wave packets separated by a. From $G(a)$, which is the spatial correlation function of each wave packet, one determines the atomic momentum distribution which is the Fourier transform of $G(a)$. The left part of the figure gives S versus a. The right part of the figure gives T_R/T versus the cooling time θ, where T_R is the recoil temperature and T the temperature of the cooled atoms determined from the width of $G(a)$. The straight line is a linear fit in agreement with the theoretical predictions of Lévy statistics. The lowest temperature, on the order of $T_R/800$, is equal to 5 nK.

In fact, it is not easy to measure such low temperatures by the usual time of flight techniques, because the resolution is then limited by the spatial extent of the initial atomic cloud. A new method has been developed [54] which consists of measuring directly the spatial correlation function of the atoms $G(a) = \int_{-\infty}^{+\infty} dz \phi^*(z + a)\phi(z)$, where $\phi(z)$ is the wave function of the atomic wave packet. This correlation function, which describes the degree of spatial coherence between two points separated by a distance a, is simply the Fourier transform of the momentum distribution $|\phi(p)|^2$. This method is analogous to Fourier spectroscopy in optics, where a narrow spectral line $I(\omega)$ is more easily inferred from the correlation function of the emitted electric field $G(\tau)$

$= \int_{-\infty}^{+\infty} dt E^*(t+\tau)E(t)$, which is the Fourier transform of $I(\omega)$. Experimentally, the measurement of $G(a)$ is achieved by letting the two coherent VSCPT wave packets fly apart with a relative velocity $2v_R = 2\hbar k/m$ during a dark period t_D, during which the VSCPT beams are switched off. During this dark period, the two wave packets get separated by a distance $a = 2v_R t_D$, and one then measures with a probe pulse a signal proportional to their overlap. Fig.8a shows the variations with t_D of such a signal S (which is in fact equal to $[1 + G(a)]/2$). From such a curve, one deduces a temperature $T \simeq T_R/625$, corresponding to $\delta p \simeq \hbar k/25$. Fig.8b shows the variations of T_R/T with the VSCPT interaction time θ. As predicted by theory (see next subsection), T_R/T varies linearly with θ and can reach values as large as 800.

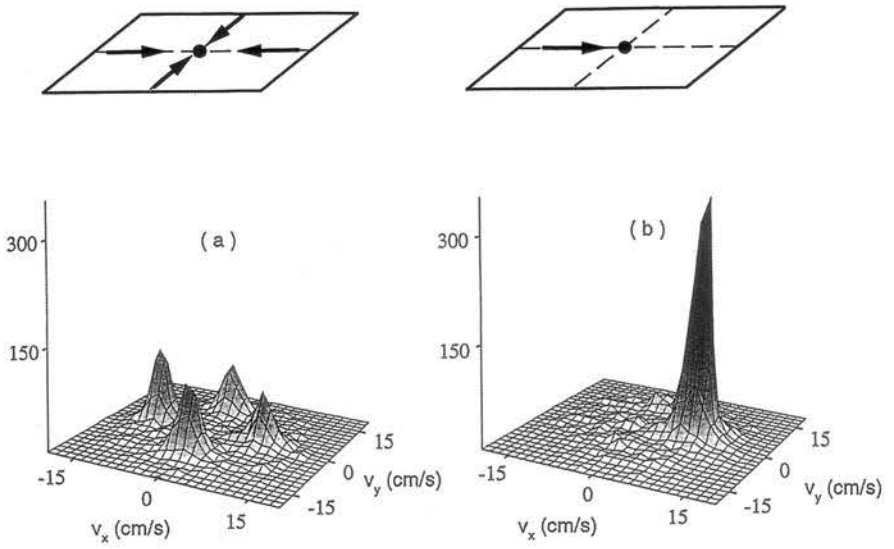

Figure 9. Two-dimensional VSCPT experiment (from reference [58]). The experimental scheme is the same as in Fig. 7, but one uses now four VSCPT beams in a horizontal plane and atoms are pumped into a linear superposition of four different momentum states giving rise to four peaks in the two-dimensional velocity distribution (a). When three of the four VSCPT laser beams are adiabatically switched off, the whole atomic population is transferred into a single wave packet (b).

VSCPT has been extended to two [55] and three [56] dimensions. For a $J_g = 1 \leftrightarrow J_e = 1$ transition, it has been shown [57] that there is a dark state which is described by the same vector field as the laser field. More precisely, if the laser field is formed by a linear superposition of N plane waves with wave vectors $\mathbf{k}_i$ ($i = 1,2,...N$) having the same modulus k, one finds that atoms are cooled in a coherent superposition of N wave packets with mean momenta $\hbar\mathbf{k}_i$ and with a momentum spread δp which becomes smaller and smaller as the interaction time θ increases. Furthermore, because of the isomorphism between the de Broglie dark state and the laser field, one can adiabatically change the laser configuration and transfer the whole atomic population into a single wave packet or two coherent wave packets chosen at will [58]. Fig. 9 shows an example of such a coherent manipulation of atomic wave packets in two dimensions. In Fig.9a, one sees the transverse velocity distribution

associated with the four wave packets obtained with two pairs of counterpropagating laser waves along the x and y-axis in a horizontal plane; Fig.9b shows the single wave packet into which the whole atomic population is transferred by switching off adiabatically three of the four VSCPT beams. Similar results have been obtained in three dimensions.

3.3 *SUBRECOIL LASER COOLING AND LÉVY STATISTICS*

Quantum Monte Carlo simulations using the delay function [59, 60] have provided new physical insight into subrecoil laser cooling [61]. Fig.10 shows for example the random evolution of the momentum p of an atom in a $1D$-VSCPT experiment. Each vertical discontinuity corresponds to a spontaneous emission process during which p changes in a random way. Between two successive jumps, p remains constant. It clearly appears that the random walk of the atom in velocity space is anomalous and dominated by a few rare events whose duration is a significant fraction of the total interaction time. A simple analysis shows that the distribution $P(\tau)$ of the trapping times τ in a small trapping zone near $v = 0$ is a broad distribution which falls as a power-law in the wings. These wings decrease so slowly that the average value $\langle\tau\rangle$ of τ (or the variance) can diverge. In such cases, the central limit theorem (CLT) can obviously no longer be used for studying the distribution of the total trapping time after N entries in the trapping zone separated by N exits.

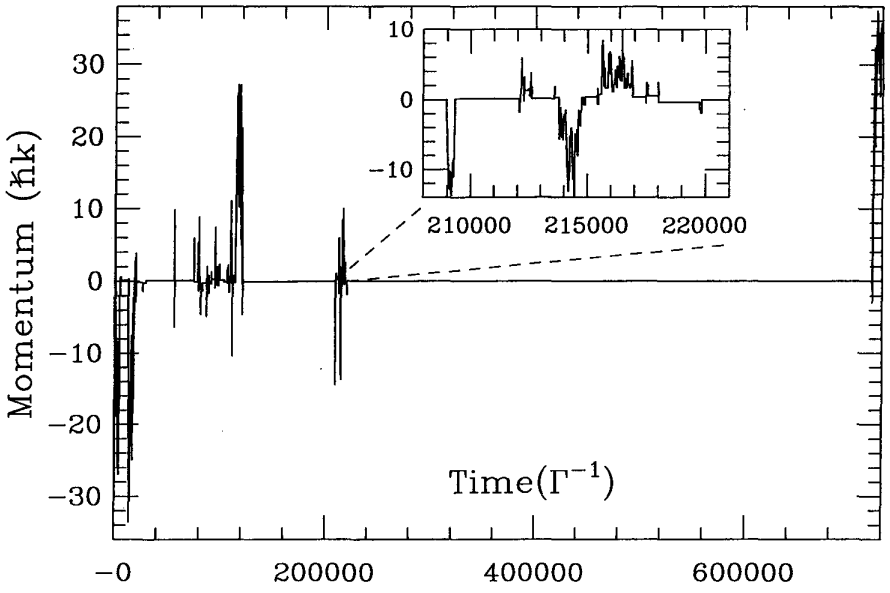

Figure 10. Monte Carlo wave function simulation of one-dimensional VSCPT (from reference [61]). Momentum p characterizing the cooled atoms versus time. Each vertical discontinuity corresponds to a spontaneous emission jump during which p changes in a random way. Between two successive jumps, p remains constant. The inset shows a zoomed part of the sequence.

It is possible to extend the CLT to broad distributions with power-law wings [62, 63]. We have applied the corresponding statistics, called "Lévy statistics", to subrecoil cooling and shown that one can obtain in this way a better understanding of the physical processes as well as quantitative analytical predictions for the asymptotic properties of the cooled atoms in the limit when the interaction time θ tends to infinity [61, 64]. For example, one predicts in this way that the temperature decreases as $1/\theta$ when $\theta \to \infty$, and that the wings of the momentum distribution decrease as $1/p^2$, which shows that the shape of the momentum distribution is closer to a Lorentzian than a Gaussian. This is in agreement with the experimental observations represented in Fig.8. (The fit in Fig.8a is an exponential, which is the Fourier transform of a Lorentzian).

One important feature revealed by this theoretical analysis is the non-ergodicity of the cooling process. Regardless of the interaction time θ, there are always atomic evolution times (trapping times in the small zone of Fig.5a around $v = 0$) which can be longer than θ. Another advantage of such a new approach is that it allows the parameters of the cooling lasers to be optimized for given experimental conditions. For example, by using different shapes for the laser pulses used in one-dimensional subrecoil Raman cooling, it has been possible to reach for Cesium atoms temperatures as low as 3 nK [65].

4. A FEW EXAMPLES OF APPLICATIONS

The possibility of trapping atoms and cooling them at very low temperatures, where their velocity can be as low as a few mm/s, has opened the way to a wealth of applications. Ultracold atoms can be observed during much longer times, which is important for high resolution spectroscopy and frequency standards. They also have very long de Broglie wavelengths, which has given rise to new research fields, such as atom optics, atom interferometry and Bose-Einstein condensation of dilute gases. It is impossible to discuss here all these developments. We refer the reader to recent reviews such as [5]. We will just describe in this section a few examples of applications which have been recently investigated by our group in Paris.

4.1 *CESIUM ATOMIC CLOCKS*

Cesium atoms cooled by Sisyphus cooling have an effective temperature on the order of 1 μK, corresponding to a r.m.s. velocity of 1 cm/s. This allows them to spend a longer time T in an observation zone where a microwave field induces resonant transitions between the two hyperfine levels g_1 and g_2 of the ground state. Increasing T decreases the width $\Delta\nu \sim 1/T$ of the microwave resonance line whose frequency is used to define the unit of time. The stability of atomic clocks can thus be considerably improved by using ultracold atoms [66. 67].

In usual atomic clocks, atoms from a thermal cesium beam cross two microwave cavities fed by the same oscillator. The average velocity of the atoms is several hundred m/s, the distance between the two cavities is on the

order of 1 m. The microwave resonance between g_1 and g_2 is monitored and is used to lock the frequency of the oscillator to the center of the atomic line. The narrower the resonance line, the more stable the atomic clock. In fact, the microwave resonance line exhibits Ramsey interference fringes whose width $\Delta\nu$ is determined by the time of flight T of the atoms from one cavity to another. For the longest devices, T, which can be considered as the observation time, can reach 10 ms, leading to values of $\Delta\nu \sim 1/T$ on the order of 100 Hz.

Much narrower Ramsey fringes, with sub-Hertz linewidths can be obtained in the so-called "Zacharias atomic fountain" [68]. Atoms are captured in a magneto-optical trap and laser cooled before being launched upwards by a laser pulse through a microwave cavity. Because of gravity they are decelerated, they return and fall back, passing a second time through the cavity. Atoms therefore experience two coherent microwave pulses, when they pass through the cavity, the first time on their way up, the second time on their way down. The time interval between the two pulses can now be on the order of 1 sec, *i.e.* about two orders of magnitude longer than with usual clocks. Atomic fountains have been realized for sodium [69] and cesium [70]. A short-term relative frequency stability of $1.3 \times 10^{-13}\tau^{-1/2}$, where τ is the integration time, has been recently measured for a one meter high Cesium fountain [71, 72]. For $\tau = 10^4 s$, $\Delta\nu/\nu \sim 1.3 \times 10^{-15}$ and for $\tau = 3 \times 10^4 s$, $\Delta\nu/\nu \sim 8 \times 10^{-16}$ has been measured. In fact such a stability is most likely limited by the Hydrogen maser which is used as a reference source and the real stability, which could be more precisely determined by beating the signals of two fountain clocks, is expected to reach $\Delta\nu/\nu \sim 10^{-16}$ for a one day integration time. In addition to the stability, another very important property of a frequency standard is its accuracy. Because of the very low velocities in a fountain device, many systematic shifts are strongly reduced and can be evaluated with great precision. With an accuracy of 2×10^{-15}, the BNM-LPTF fountain is presently the most accurate primary standard [73]. A factor 10 improvement in this accuracy is expected in the near future.

To increase the observation time beyond one second, a possible solution consists of building a clock for operation in a reduced gravity environment. Such a microgravity clock has been recently tested in a jet plane making parabolic flights. A resonance signal with a width of 7 Hz has been recorded in a $10^{-2}g$ environment. This width is twice narrower than that produced on earth in the same apparatus. This clock prototype (see Fig.11) is a compact and transportable device which can be also used on earth for high precision frequency comparison.

Atomic clocks working with ultracold atoms could not only provide an improvement of positioning systems such as the GPS. They could be also used for fundamental studies. For example, one could build two fountains clocks, one with cesium and one with rubidium, in order to measure with a high accuracy the ratio between the hyperfine frequencies of these two atoms. Because of relativistic corrections, the hyperfine splitting is a function of $Z\alpha$ where α is the fine structure constant and Z is the atomic number [74]. Since Z is not the same for cesium and rubidium, the ratio of the two hyperfine

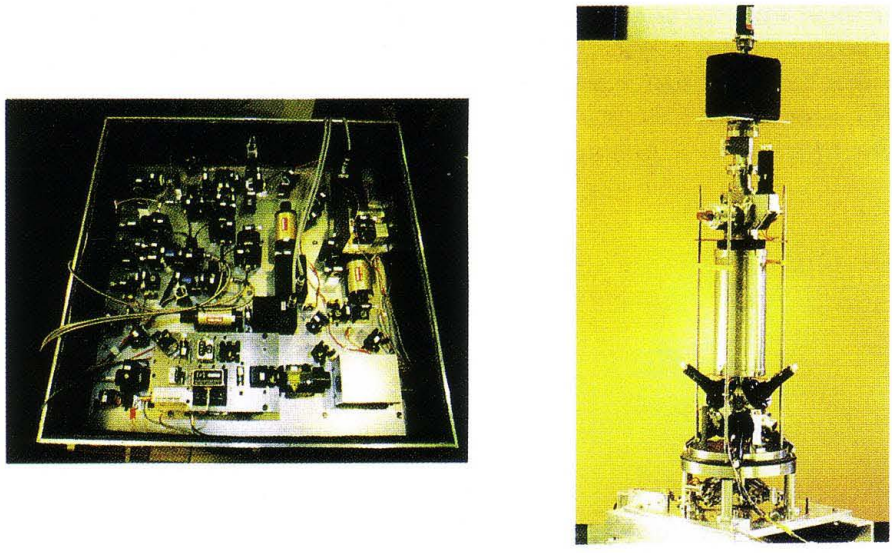

Figure 11. The microgravity clock prototype. The left part is the 60 cm × 60 cm × 15 cm optical bench containing the diode laser sources and the various optical components. The right part is the clock itself (about one meter long) containing the optical molasses, the microwave cavity and the detection region.

structures depends on α. By making several measurements of this ratio over long periods of time, one could check Dirac's suggestion concerning a possible variation of α with time. The present upper limit for $\dot{\alpha}/\alpha$ in laboratory tests [74] could be improved by two orders of magnitude.

Another interesting test would be to measure with a higher accuracy the gravitational red shift and the gravitational delay of an electromagnetic wave passing near a large mass (Shapiro effect [75]).

4.2 *GRAVITATIONAL CAVITIES FOR NEUTRAL ATOMS*

We have already mentioned in section 1.3 the possibility of making atomic mirrors for atoms by using blue detuned evanescent waves at the surface of a piece of glass. Concave mirrors (Fig.12a) are particularly interesting because the transverse atomic motion is then stable if atoms are released from a point located below the focus of the mirror. It has been possible in this way to observe several successive bounces of the atoms (Fig.12b) and such a system can be considered as a "trampoline for atoms" [37]. In such an experiment, it is a good approximation to consider atoms as classical particles bouncing off a concave mirror. In a quantum mechanical description of the experiment, one must consider the reflection of the atomic de Broglie waves by the mirror. Standing de Broglie waves can then be introduced for such a "gravitational cavity", which are quite analogous to the light standing waves for a Fabry-Perot cavity [76]. By modulating at frequency $\Omega/2\pi$ the intensity of the evanescent wave which forms the atomic mirror, one can produce the equivalent of a vibrating mirror for de Broglie waves. The reflected waves thus have a modulated Doppler shift. The corresponding frequency modulation

of these waves has been recently demonstrated [77] by measuring the energy change ΔE of the bouncing atom, which is found to be equal to $n\hbar\Omega$, where $n = 0, \pm 1, \pm 2, \ldots$ (Figs.12c and d). The discrete nature of this energy spectrum is a pure quantum effect. For classical particles bouncing off a vibrating mirror, ΔE would vary continuously in a certain range.

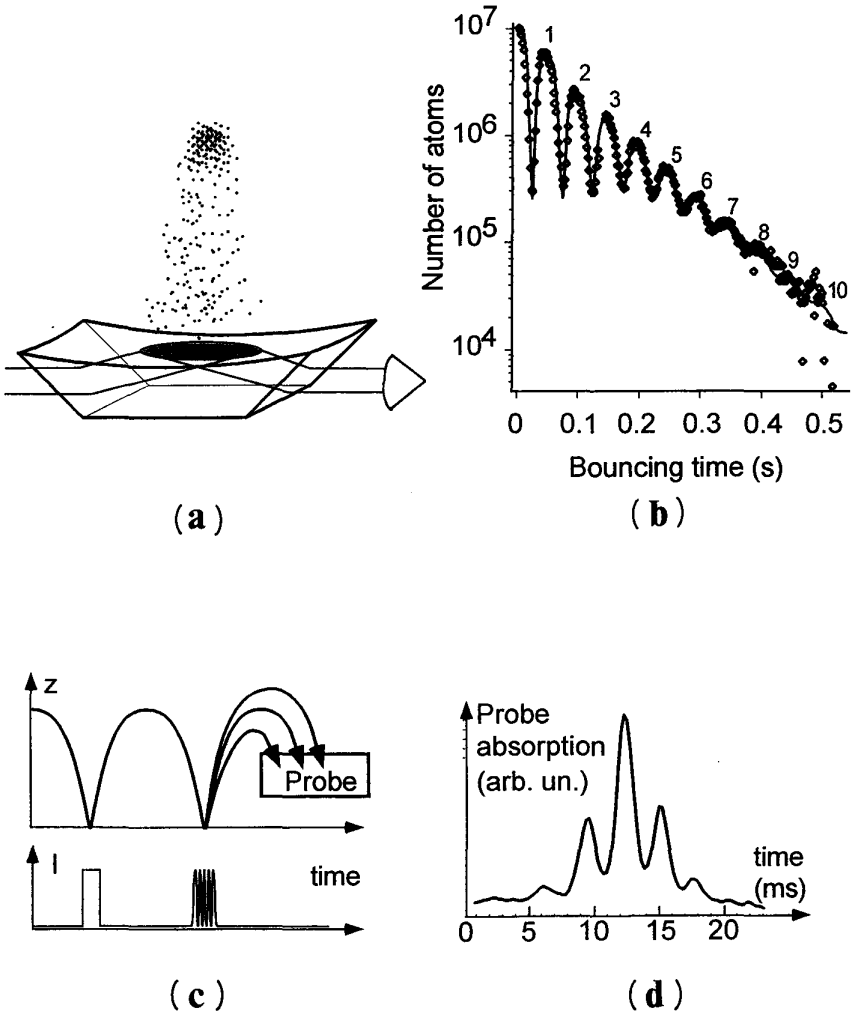

Figure 12. Gravitational cavity for neutral atoms (from references [37] and [77]). Trampoline for atoms (a) – Atoms released from a magneto-optical trap bounce off a concave mirror formed by a blue detuned evanescent wave at the surface of a curved glass prism. Number of atoms at the initial position of the trap versus time after the trap has been switched off (b). Ten successive bounces are visible in the figure. Principle of the experiment demonstrating the frequency modulation of de Broglie waves (c). The upper trace gives the atomic trajectories (vertical position z versus time). The lower trace gives the time dependence of the intensity I of the evanescent wave. The first pulse is used for making a velocity selection. The second pulse is modulated in intensity. This produces a vibrating mirror giving rise to a frequency modulated reflected de Broglie wave which consists in a carrier and sidebands at the modulation frequency. The energy spectrum of the reflected particles is thus discrete so that the trajectories of the reflected particles form a discrete set. This effect is detected by looking at the time dependence of the absorption of a probe beam located above the prism (d).

4.3 *BLOCH OSCILLATIONS*

In the subrecoil regime where δp becomes smaller than $\hbar k$, the atomic coherence length $h/\delta p$ becomes larger than the optical wavelength $\lambda = h/\hbar k = 2\pi/k$ of the lasers used to cool the atom. Consider then such an ultracold atom in the periodic light shift potential produced by a non resonant laser standing wave. The atomic de Broglie wave is delocalized over several periods of the periodic potential, which means that one can prepare in this way quasi-Bloch states. By chirping the frequency of the two counterpropagating laser waves forming the standing wave, one can produce an accelerated standing wave. In the rest frame of this wave, atoms thus feel a constant inertial force in addition to the periodic potential. They are accelerated and the de Broglie wavelength $\lambda_{dB} = h/M\langle v\rangle$ decreases. When $\lambda_{dB} = \lambda_{Laser}$, the de Broglie wave is Bragg-reflected by the periodic optical potential. Instead of increasing linearly with time, the mean velocity $\langle v\rangle$ of the atoms oscillates back and forth. Such Bloch oscillations, which are a textbook effect of solid-state physics, are more easily observed with ultracold atoms than with electrons in condensed matter because the Bloch period can be much shorter than the relaxation time for the coherence of de Broglie waves (in condensed matter, the relaxation processes due to collisions are very strong). Fig.13 shows an example of Bloch oscillations [78] observed on cesium atoms cooled by the improved subrecoil Raman cooling technique described in [65].

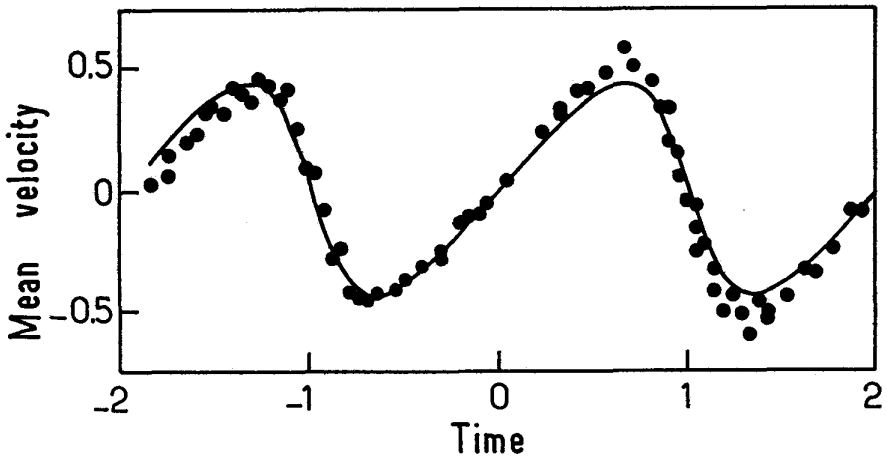

Figure 13. Bloch oscillations of atoms in a periodic optical potential (from reference [78]. Mean velocity (in units of the recoil velocity) versus time (in units of half the Bloch period) for ultracold cesium atoms moving in a periodic optical potential and submitted in addition to a constant force.

5. CONCLUSION

We have described in this paper a few physical mechanisms allowing one to manipulate neutral atoms with laser light. Several of these mechanisms can be simply interpreted in terms of resonant exchanges of energy, angular and linear momentum between atoms and photons. A few of them, among the

most efficient ones, result from a new way of combining well known physical effects such as optical pumping, light shifts, coherent population trapping. We have given two examples of such cooling mechanisms, Sisyphus cooling and subrecoil cooling, which allow atoms to be cooled in the microKelvin and nanoKelvin ranges. A few possible applications of ultracold atoms have been also reviewed. They take advantage of the long interaction times and long de Broglie wavelengths which are now available with laser cooling and trapping techniques.

One can reasonably expect that further progress in this field will be made in the near future and that new applications will be found. Concerning fundamental problems, two directions of research at least look promising. First, a better control of "pure" situations involving a small number of atoms in well-defined states exhibiting quantum features such as very long spatial coherence lengths or entanglement. In that perspective, atomic, molecular and optical physics will continue to play an important role by providing a "testing bench" for improving our understanding of quantum phenomena. A second interesting direction is the investigation of new systems, such as Bose condensates involving a macroscopic number of atoms in the same quantum state. One can reasonably hope that new types of coherent atomic sources (sometimes called "atom lasers") will be realized, opening the way to interesting new possibilities.

It is clear finally that all the developments which have occurred in the field of laser cooling and trapping are strengthening the connections which can be established between atomic physics and other branches of physics, such as condensed matter or statistical physics. The use of Lévy statistics for analyzing subrecoil cooling is an example of such a fruitful dialogue. The interdisciplinary character of the present researches on the properties of Bose condensates is also a clear sign of the increase of these exchanges.

REFERENCES

[1] A. Kastler, J. Phys. Rad. **11,** 255 (1950).
[2] A. Ashkin, Science, **210,** 1081 (1980).
[3] V.S. Letokhov and V.G. Minogin, Phys.Reports, **73,** 1 (1981).
[4] S. Stenholm, Rev.Mod.Phys. **58,** 699 (1986).
[5] C.S. Adams and E. Riis, Prog. Quant. Electr. **21,** 1 (1997).
[6] C. Cohen-Tannoudji and W. Phillips, Physics Today **43,** No 10, 33 (1990).
[7] W. Heitler, "The quantum theory of radiation", 3rd ed. (Clarendon Press, Oxford, 1954).
[8] J-P. Barrat and C.Cohen-Tannoudji, J.Phys.Rad. **22,** 329 and 443 (1961).
[9] C.Cohen-Tannoudji , Ann. Phys. Paris **7,** 423 and 469 (1962).
[10] C. Cohen-Tannoudji, J. Dupont-Roc and G. Grynberg, "Atom-photon interactions–Basic processes and applications", (Wiley, New York, 1992).
[11] S.H. Autler and C.H. Townes, Phys.Rev. **100,** 703 (1955).
[12] C. Cohen-Tannoudji, C.R.Acad.Sci.(Fr) **252,** 394 (1961).
[13] C. Cohen-Tannoudji and J. Dupont-Roc, Phys.Rev. **A5,** 968 (1972).
[14] W.D.Phillips and H.Metcalf, Phys.Rev.Lett. **48,** 596 (1982).
[15] J.V.Prodan, W.D.Phillips and H.Metcalf, Phys.Rev.Lett. **49,** 1149 (1982).
[16] W. Ertmer, R. Blatt, J.L. Hall and M. Zhu, Phys.Rev.Lett. **54,** 996 (1985).

[17] G.A. Askarian, Zh.Eksp.Teor.Fiz. **42,** 1567 (1962) [Sov.Phys.JETP, 15, 1088 (1962)].
[18] C. Cohen-Tannoudji, "Atomic motion in laser light", in "Fundamental systems in quantum optics", J. Dalibard, J.-M. Raimond, and J. Zinn-Justin eds, Les Houches session LIII (1990), (North-Holland, Amsterdam 1992) p.1.
[19] J. Dalibard and C. Cohen-Tannoudji, J.Opt.Soc.Am. **B2,** 1707 (1985).
[20] T.W. Hänsch and A.L. Schawlow, Opt. Commun. **13,** 68 (1975).
[21] D.Wineland and H.Dehmelt, Bull.Am.Phys.Soc. **20,** 637 (1975).
[22] S. Chu, L. Hollberg, J.E. Bjorkholm, A. Cable and A. Ashkin, Phys. Rev. Lett. **55,** 48 (1985).
[23] V.S. Letokhov, V.G. Minogin and B.D. Pavlik, Zh.Eksp.Teor.Fiz. **72,** 1328 (1977) [Sov.Phys.JETP, **45,** 698 (1977)].
[24] D.J. Wineland and W. Itano, Phys.Rev. **A20,** 1521 (1979).
[25] J.P. Gordon and A. Ashkin, Phys.Rev. **A21,** 1606 (1980).
[26] P.D. Lett, R.N. Watts, C.I. Westbrook, W. Phillips, P.L. Gould and H.J. Metcalf, Phys. Rev. Lett. **61,** 169 (1988).
[27] E.L. Raab, M. Prentiss, A. Cable, S. Chu and D.E. Pritchard, Phys.Rev.Lett. **59,** 2631 (1987).
[28] C. Monroe, W. Swann, H. Robinson and C.E. Wieman, Phys.Rev.Lett. **65,** 1571 (1990).
[29] S. Chu, J.E. Bjorkholm, A. Ashkin and A. Cable, Phys.Rev.Lett. **57,** 314 (1986).
[30] C.S. Adams, H.J. Lee, N. Davidson, M. Kasevich and S. Chu, Phys. Rev. Lett. **74,** 3577 (1995).
[31] A. Kuhn, H. Perrin, W. Hänsel and C. Salomon, OSA TOPS on Ultracold Atoms and BEC, 1996, Vol. 7, p.58, Keith Burnett (ed.), (Optical Society of America, 1997).
[32] V.S. Letokhov, Pis'ma.Eksp.Teor.Fiz. **7,** 348 (1968) [JETP Lett., **7,** 272 (1968)].
[33] C. Salomon, J. Dalibard, A. Aspect, H. Metcalf and C. Cohen-Tannoudji, Phys. Rev. Lett. **59,** 1659 (1987).
[34] R.J. Cook and R.K. Hill, Opt. Commun. **43,** 258 (1982)
[35] V.I. Balykin, V.S. Letokhov, Yu. B. Ovchinnikov and A.I. Sidorov, Phys. Rev. Lett. **60,** 2137 (1988).
[36] M.A. Kasevich, D.S. Weiss and S. Chu, Opt. Lett. **15,** 607 (1990).
[37] C.G. Aminoff, A.M. Steane, P. Bouyer, P. Desbiolles, J. Dalibard and C. Cohen-Tannoudji, Phys. Rev. Lett. **71,** 3083 (1993).
[38] J. Dalibard and C. Cohen-Tannoudji, J. Opt. Soc. Am. **B6,** 2023 (1989).
[39] P.J. Ungar, D.S. Weiss, E. Riis and S. Chu, JOSA **B6,** 2058 (1989).
[40] C. Salomon, J. Dalibard, W. Phillips, A. Clairon and S. Guellati, Europhys. Lett. **12,** 683 (1990).
[41] Y. Castin, These de doctorat, Paris (1991).
[42] Y. Castin and K. Mølmer, Phys. Rev. Lett. **74,** 3772 (1995).
[43] Y. Castin and J. Dalibard, Europhys.Lett. **14,** 761 (1991).
[44] P. Verkerk, B. Lounis, C. Salomon, C. Cohen-Tannoudji, J.-Y. Courtois and G. Grynberg, Phys. Rev. Lett. **68,** 3861 (1992).
[45] P.S. Jessen, C. Gerz, P.D. Lett, W.D. Phillips, S.L. Rolston, R.J.C. Spreeuw and C.I. Westbrook, Phys. Rev. Lett. **69,** 49 (1992).
[46] G. Grynberg and C. Triché, in Proceedings of the International School of Physics "Enrico Fermi", Course CXXXI, A. Aspect, W. Barletta and R. Bonifacio (Eds), p.243, IOS Press, Amsterdam (1996); A. Hemmerich, M. Weidemüller and T.W. Hänsch, same Proceedings, p.503.
[47] P.S. Jessen and I.H. Deutsch, in Advances in Atomic, Molecular and Optical Physics, **37,** 95 (1996), ed. by B. Bederson and H. Walther.
[48] A. Aspect, E. Arimondo, R. Kaiser, N. Vansteenkiste, and C. Cohen-Tannoudji, Phys. Rev. Lett. **61,** 826 (1988).
[49] M. Kasevich and S. Chu, Phys. Rev. Lett. **69,** 1741 (1992).
[50] Alzetta G., Gozzini A., Moi L., Orriols G., Il Nuovo Cimento **36B,** 5 (1976).
[51] Arimondo E., Orriols G., Lett. Nuovo Cimento **17,** 333 (1976).

[52] A. Aspect, E. Arimondo, R. Kaiser, N. Vansteenkiste, and C. Cohen-Tannoudji, J. Opt. Soc. Am. **B6**, 2112 (1989).
[53] F. Bardou, B. Saubamea, J. Lawall, K. Shimizu, O. Emile, C. Westbrook, A. Aspect, C. Cohen-Tannoudji, C. R. Acad. Sci. Paris **318,** 877-885 (1994).
[54] B. Saubamea, T.W. Hijmans, S. Kulin, E. Rasel, E. Peik, M. Leduc and C. Cohen-Tannoudji, Phys.Rev.Lett. **79,** 3146 (1997).
[55] J. Lawall, F. Bardou, B. Saubamea, K. Shimizu, M. Leduc, A. Aspect and C. Cohen-Tannoudji, Phys. Rev. Lett. **73,** 1915 (1994).
[56] J. Lawall, S. Kulin, B. Saubamea, N. Bigelow, M. Leduc and C. Cohen-Tannoudji, Phys. Rev. Lett. **75,** 4194 (1995).
[57] M.A. Ol'shanii and V.G. Minogin, Opt. Commun. **89,** 393 (1992).
[58] S. Kulin, B. Saubamea, E. Peik, J. Lawall, T.W. Hijmans, M. Leduc and C .Cohen-Tannoudji, Phys. Rev. Lett. **78**, 4185 (1997).
[59] C. Cohen-Tannoudji and J. Dalibard, Europhys. Lett. **1,** 441 (1986).
[60] P. Zoller, M. Marte and D.F. Walls, Phys. Rev. **A35,** 198 (1987).
[61] **F. Bardou, J.-P. Bouchaud, O. Emile, A. Aspect and C. Cohen-Tannoudji, Phys. Rev. Lett. 72, 203 (1994).**
[62] B.V. Gnedenko and A.N. Kolmogorov, "Limit distributions for sum of independent random variables" (Addison Wesley, Reading, MA, 1954).
[63] J.P. Bouchaud and A. Georges, Phys. Rep. **195,** 127 (1990).
[64] F. Bardou, Ph. D. Thesis, University of Paris XI, Orsay (1995).
[65] J. Reichel, F. Bardou, M. Ben Dahan, E. Peik, S. Rand, C. Salomon and C. Cohen-Tannoudji, Phys. Rev. Lett. **75,** 4575 (1995).
[66] K. Gibble and S. Chu, Metrologia, **29,** 201 (1992).
[67] S.N. Lea, A. Clairon, C. Salomon, P. Laurent, B. Lounis, J. Reichel, A. Nadir, and G. Santarelli, Physica Scripta **T51,** 78 (1994).
[68] J. Zacharias, Phys.Rev. **94,** 751 (1954). See also : N. Ramsey, Molecular Beams, Oxford University Press, Oxford, 1956.
[69] M. Kasevich, E. Riis, S. Chu and R. de Voe, Phys. Rev. Lett. **63,** 612 (1989).
[70] A. Clairon, C. Salomon, S. Guellati and W.D. Phillips, Europhys. Lett. **16,** 165 (1991).
[71] S. Ghezali, Ph. Laurent, S.N. Lea and A. Clairon, Europhys. Lett. **36,** 25 (1996).
[72] S. Ghezali, Thèse de doctorat, Paris (1997).
[73] E. Simon, P. Laurent, C. Mandache and A. Clairon, Proceedings of EFTF 1997, Neuchatel, Switzerland.
[74] J. Prestage, R. Tjoelker and L. Maleki, Phys. Rev. Lett. **74,** 3511 (1995).
[75] I.I.Shapiro, Phys. Rev. Lett. **13,** 789 (1964).
[76] H. Wallis, J. Dalibard and C. Cohen-Tannoudji, Appl. Phys. **B54,** 407 (1992).
[77] A. Steane, P. Szriftgiser, P. Desbiolles and J. Dalibard, Phys. Rev. Lett. **74,** 4972 (1995).
[78] M. Ben Dahan, E. Peik, J. Reichel, Y. Castin and C. Salomon, Phys. Rev. Lett. **76,** 4508 (1996).